

A quantum emitter coated with graphene interacting in the strong coupling regime

Mehmet Günay^{(a)*}, Vasilios Karanikolas^{(a)†}, Ramazan Sahin^(b), Alpan Bek^(c), and Mehmet Emre Tasgin^(a)

^(a)*Institute of Nuclear Sciences, Hacettepe University, 06800 Ankara, Turkey*

^(b)*Vocational School of Technical Sciences, Akdeniz University, 07058 Antalya, Turkey and*

^(c)*Department of Physics, Middle East Technical University, 06800 Ankara, Turkey*

We investigate the optical response of a graphene spherical shell which has a semi-conducting material core through their absorption spectrum. The semi-conducting material is described by a Lorentzian expression, which approximates the optical response of a quantum emitter. We present the tunability of the localized plasmon resonance of the graphene sphere by changing the value of its chemical potential and radius. The semi-conducting sphere supports a localized exciton mode, appearing as a maximum in its absorption spectrum. When the localized exciton mode energy, of the semi-conducting sphere, matches the localized plasmon resonance of the graphene, a splitting is observed in the absorption spectrum. This splitting is due to the interaction of the localized exciton mode with the plasmon mode of the graphene sphere, where a splitting of 80 meV is observed close to the telecommunication wavelength of 1550 nm. Using a theoretical model, we explain the modulations in the intensity of the hybrid exciton-plasmon mode, which can be controlled by the radius and the chemical potential of the graphene sphere and the localized exciton mode of the semi-conducting sphere. The results presented here can be used for designing broadband tunable photonic devices.

I. INTRODUCTION

Graphene is a material with superior optical, electronic and mechanical properties [1–5]. Graphene can be used for replacing noble metals (mainly Au and Ag) for applications operating near to far infrared wavelengths [6]. Graphene possesses an advantage over noble metals because it has smaller material losses [7] and also its optical properties are tunable [8], thus allowing the design of multipurpose applications [9–11].

In recent years, graphene has also been recognized as a promising active material for supercapacitors. Studies showed that having large surface area is essential for such applications [12, 13]. In this direction, it is suggested to use a spherical geometry (graphene nano-balls) to increase the surface area. Lee et al. [14] showed that a graphene mesoporous, with a mean mesopore diameter of 4.27 nm, can be fabricated via chemical vapor deposition technique. Additionally, self-crystallized graphene and graphite nanoballs has been recently demonstrated via Ni vapor-assisted growth [15]. However, these studies mainly focus on electrical properties of such structures. It is also intriguing to study the optical applications of the graphene spherical shell (GSS) structures. In Refs. [16, 17], the electromagnetic response of charged spherical shells has been studied in terms of their plasmonic properties.

Graphene plasmons (GPs) emerge by applying a voltage or by electrostatic doping, and can trap the incident light in small volumes [18, 19]. Providing incredible potential in a vast amount of applications, such as sensing [20], switching [8], and metamaterials [21]. Placing

a quantum emitter (QE), such as quantum dot (QD), in close proximity to a graphene nanostructure can yield strong interaction [18] and modulations in optical properties. Usually the interactions between QE placed in a nanostructured environment are described through investigating the QE's lifetime, calculating the Purcell factor [18]. For such simulations the QE-nanostructure interaction is described in terms of the non-Hermitian description of the quantum electrodynamics, and the QE is approached as a point dipole source. Moreover, the interaction between QEs and an infinite graphene layer has been investigated experimentally by measuring the relaxation rate for varying the distance between them [22] and varying the chemical potential value of the graphene layer [23]. The QEs used are erbium ions with a transition energy close to the telecommunication wavelength, where the graphene nanostructures can have a plasmonic response for specific chemical potential values. Moreover, there are molecular and quantum dots emitters also operating to infrared wavelength [24, 25].

In this work, we study optical response of GPs for the spherical shell geometry, and show that GP resonance can be tuned by changing its radius or chemical potential. We also investigate its interaction with a QE, where it is approached as a semi-conducting sphere. We present a "proof of principal" demonstration that strong coupling between GSS and QE can be achieved in a single QE limit. To show this we use the MNPBEM package [26], which solves the Maxwell equations in 3D. We observe an 80 meV splitting of the hybrid modes when the QE is resonant to the GP. We also observe that such strong coupling holds when particles becomes off-resonant by tuning chemical potential of the GSS. Having this type of hybrid modes can be valuable for sensing applications, since one of the hybrid modes has sharper linewidth providing high resolution. And tunability of this mode makes it even more attractive. The consistent results are obtained

* gunaymehmt@gmail.com

† karanikv@tcd.ie

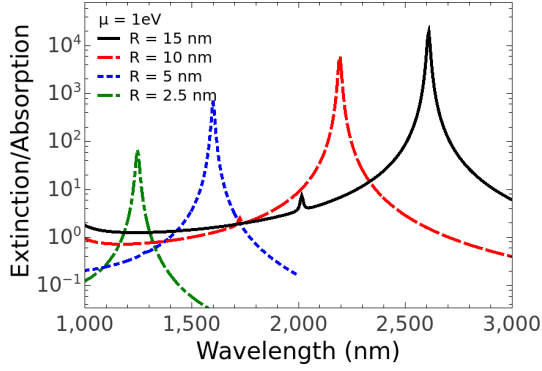


FIG. 1. Absorption spectrum of the GSS, varying the excitation wavelength. We keep fixed the value of the chemical potential, $\mu = 1$ eV, of the GSS, for different values of its radius, $R = 2.5$ nm, 5 nm, 10 nm and 15 nm.

with a basic analytical model presented here. With this model, we discuss the steady state behavior of the hybrid modes depending on the system parameters.

The paper is organized as follows. In Sec. II we present results regarding the absorption spectrum of the GSS, the semi-conducting sphere and the full case, combination of a QE with a GSS. In Sec. III we describe the theoretical model and derive an effective Hamiltonian for a two-level system coupled to GPs. We derive the equations of motion for the system and obtain a single equation for the plasmon amplitude in the steady-state. Sec. IV contains our conclusions.

II. ELECTROMAGNETIC SIMULATIONS OF THE ABSORPTION OF A GRAPHENE COATED SEMI-CONDUCTING SPHERE

We consider a GSS and its optical response is given through the surface conductivity, which is used for the calculation of its absorption cross sections. When the absorption peak of the QE matches the GP resonance, we observe a splitting in the absorption band due to the interaction between the exciton polariton mode, of the semi-conducting sphere, with the localized surface GP mode, supported by the GSS. This splitting is connected with the energy exchange between the two modes. Due to the large splitting the system enters the strong coupling regime, where a splitting of 80 meV between the hybrid-modes is observed [27]. These type of collective modes have been also named as plexcitons [28]. We stress out that the QE coated with GSS has been experimentally demonstrated [29]. In this section, we start by presenting the mathematical framework and the expressions that give the dielectric permittivities of the GSS and of the semi-conducting QE. Next we present results regarding the absorption spectrum of the GSS, the QE and the full case of QE with a GSS coating.

The optical response of graphene is given by the value of the in-plane conductivity, σ , in the random phase

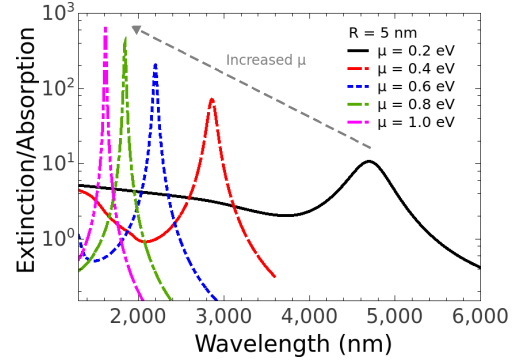


FIG. 2. Extinction/absorption spectrum of the GSS, varying the excitation wavelength. We keep fixed the radius, $R = 5$ nm, of the GSS, for different values of chemical potential, $\mu = 0.2$ eV, 0.4 eV, 0.6 eV, 0.8 eV and 1.0 eV.

approximation [30, 31]. This quantity is mainly determined by electron-hole pair excitations, which can be divided into intraband and interband transitions $\sigma = \sigma_{\text{intra}} + \sigma_{\text{inter}}$. It depends on the chemical potential (μ), the temperature (T), and the scattering energy (E_S) values [32].

The intraband term σ_{intra} describes a Drude modes response, corrected for scattering by impurities through a term containing τ , the relaxation time. The relaxation time, τ , causes the plasmons to acquire a finite lifetime and is influenced by several factors, such as collisions with impurities, coupling to optical phonons and finite-size effects. In this paper we consider room temperature $T = 300$ K and a value of the relaxation time of $\tau = 1$ ps and we vary the value of chemical potential, μ [9].

In Fig. 1 and Fig. 2, we present the extinction spectrum of the GSS by a plane wave illumination. In both figures we observe a peak in the extinction spectrum, this peak value is due to the excitation of localized surface plasmon mode supported by the GSS. In particular, the localized surface plasmon resonances frequency is given as a solution of the equation [16]:

$$\frac{i\epsilon\omega_l}{2\pi\sigma(\omega_l)} = \left(1 + \frac{1}{2l+1}\right) \frac{l}{R}, \quad (2.1)$$

where R is the radius of the GSS, ϵ is the dielectric permittivity of the surrounding medium and the space inside the GSS and l is the resonance eigenvalue which is connected with the expansion order. Here we focus on GSS radii that $R \ll \lambda$, where λ is the excitation wavelength, thus we focus on the dipole mode $l = 1$. Since, $R \ll \lambda$, the extinction and the absorption have essentially the same value. Moreover, the localized surface plasmon resonance depends on the intraband contributions of the surface conductivity, which, in the limit $\mu/\hbar\omega \gg 1$, $\sigma(\omega) = 4ia\mu/\hbar\omega$, ignoring the plasmon lifetime. Then, the resonance wavelength of the dipole sur-

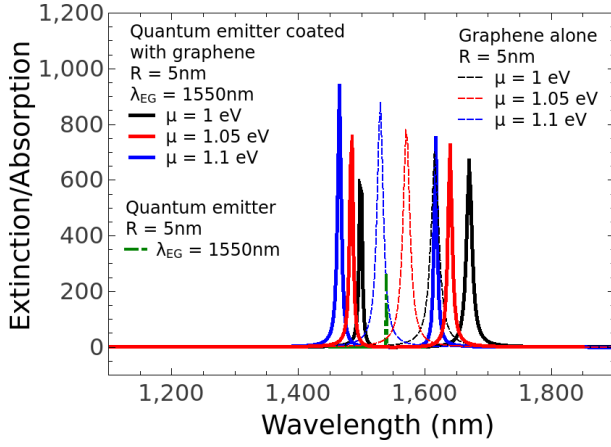


FIG. 3. Absorption spectra of the QE coated with the GSS, are presented varying the excitation wavelength. Different values of the chemical potential are considered, while the QE transition energy is $\lambda_{eg} = 1550$ nm. More details on the parameters are given in the inset.

face plasmon resonance has the value:

$$\lambda_1 = 2\pi c \sqrt{\frac{\hbar \varepsilon}{\pi a \mu}} \frac{1}{12} R. \quad (2.2)$$

In boundary element simulations, using MNPBEM [26], the GSS is modeled as a thin layer of thickness $d = 0.5$ nm, with a dielectric permittivity given by [33]

$$\varepsilon(\omega) = 1 + \frac{4\pi\sigma(\omega)}{\omega d}, \quad (2.3)$$

where the surface conductivity is given by 2.1 [9].

In Fig. 1, we present the absorption spectrum of the GSS by varying the excitation wavelength, considering different values of its radius $R = 2.5$ nm, 5 nm, 10 nm and 15 nm. We consider a fixed value for the chemical potential, $\mu = 1$ eV and observe that by increasing the radius of the GSS the surface plasmon resonance is red-shifted as is predicted by Eq. 2.2. The dipole surface plasmon resonance from Fig. 1 for $R = 10$ nm is 2190 nm and from numerically solving Eq. 2.1 is 2120 nm, validating our approach. Moreover, increasing the GSS radius the absorption strength gets higher.

In Fig. 2, we present the extinction spectrum of the GSS, for fixed radius $R = 5$ nm, varying the excitation wavelength for different values of the chemical potential, $\mu = 0.2$ eV, 0.4 eV, 0.6 eV, 0.8 eV and 1.0 eV. As the value of the chemical potential is increasing the GP resonance is blue shifted to lower wavelengths, also predicted from Eq. 2.2. The physical explanation for such behavior is that the optical gap increases as the chemical potential value increases, thus the surface plasmon resonance blue-shifts.

The optical properties of the QE are also described through its absorption spectrum. We want to stress out that we do not consider the emission of the QE and we

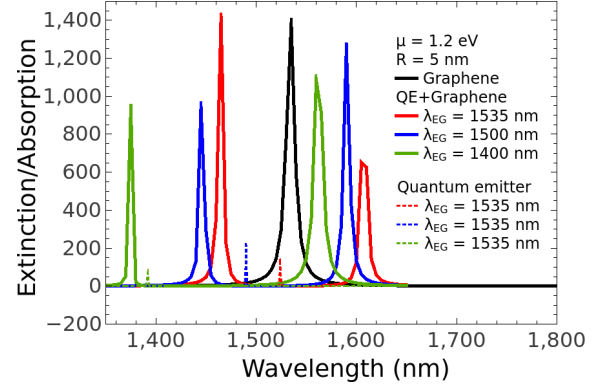


FIG. 4. Absorption spectra of the QE coated with the GSS, are presented varying the excitation wavelength. Fixed value for the chemical potential is considered, $\mu = 1.2$ eV, while different values of the transition energy of the QE are considered. More details in the inset.

model its optical response through a Lorentzian dielectric permittivity [34]

$$\varepsilon_{eg}(\omega) = \epsilon_\infty - f \frac{\omega_{eg}^2}{\omega^2 - \omega_{eg}^2 + i\gamma_{eg}\omega}, \quad (2.4)$$

where ϵ_∞ is the bulk dielectric permittivity at high frequencies, f is the oscillator strength [35, 36] and γ_{eg} is the transition linewidth, which is connected with the quality of the QE. ω_{eg} is connected with the energy from the excited to the ground state of the QE. As the sphere is composed by a semi-conducting material, supports localized exciton polariton modes. The sphere sizes considered in this paper are much smaller than the excitation wavelength and only the dipole exciton resonance is excited. In the electrostatic limit the condition for exciting the dipole localized exciton resonance is given by the $Re(\varepsilon_{eg}(\omega)) = -2\varepsilon$, where ε is the dielectric permittivity of the surrounding medium, in this paper we consider $\varepsilon = 1$. From this resonance condition it becomes apparent that changing the radius of the semi-conducting sphere does not influence its resonance wavelength, as long as $R \ll \lambda$. On the other hand, as the level spacing of the QE changes, the position of the dipole localized exciton resonance shifts accordingly.

In Fig. 3 we consider the full case in which the QE has a GSS coating. We simulate the absorption of the combined system for varying excitation wavelength. We start in Fig. 3 by considering the effect of the value of the chemical potential, μ , in the absorption of the combined system, where the value of the transition energy of the QE is fixed at $\lambda_{eg} = 1550$ nm. For the chemical potential $\mu = 1$ eV the splitting in the absorption spectrum is $\hbar\Omega = 84$ meV, where we can see that the localized exciton mode is off-resonance with the surface plasmon mode, although we can still observe a strong coupling behavior. We observe that the initial splitting blue-shifts as the value of the chemical potential μ increases.

In Fig. 4 we present the absorption of the QE coated with GSS, with $\mu = 1.2$ eV and the radius of the sphere

to be $R = 5$ nm, for varying excitation wavelength. We consider different values of the transition energy of the QE, λ_{eg} . We observe that by increasing the value of λ_{eg} the resonance of the exciton polariton mode redshifts, similarly the splitting in the extinction/absorption of the combined QE core-GSS nanosystem also redshifts. Initially for $\lambda_{eg} = 1400$ nm the exciton polariton and the GP modes are not interacting as the value of the QE transition wavelength increases then the exciton resonance of the QE overlaps with the GPs, then a splitting appears. For $\lambda_{eg} = 1400$ nm the absorption spectrum shows that the exciton and plasmon polariton modes are shifted from their initial values due to the modification of the local refractive index environment.

III. THE ANALYTICAL MODEL

In the following section, we derive the effective Hamiltonian for the GPs coupled to a QE and derive the equations of motion. We consider the QE as a two level system [34] with level spacing $\omega_{eg} = 2\pi c/\lambda_{eg}$. In the steady state, we obtain a single equation. We show that by using this equation one can have a better understanding on the parameters of the combined system.

We consider the dynamics of the total system as follows. The incident light (ε_L) with optical frequency $\omega = 2\pi c/\lambda$ excites a GP (\hat{a}_{GP}), which is coupled to a QE. The Hamiltonian of the system can be written as the sum of the energy of the QE and GP ($\omega_{GP} = 2\pi c/\lambda_{GP}$) oscillations (\hat{H}_0) and the energy transferred by the pump source (\hat{H}_L)

$$\hat{H}_0 = \hbar\omega_{GP}\hat{a}_{GP}^\dagger\hat{a}_{GP} + \hbar\omega_{eg}|e\rangle\langle e| \quad (3.1)$$

$$\hat{H}_L = i\hbar(\varepsilon_L\hat{a}_{GP}^\dagger e^{-i\omega t} - h.c) \quad (3.2)$$

and the interaction of the QE with the GP modes (\hat{H}_{int})

$$\hat{H}_{int} = \hbar\{\Omega_R^*\hat{a}_{GP}^\dagger|g\rangle\langle e| + \Omega_R|e\rangle\langle g|\hat{a}_{GP}\}, \quad (3.3)$$

where the parameter Ω_R , in units of frequency, is the coupling strength between GP and the QE. $|g\rangle$ ($|e\rangle$) is the ground (excited) state of the QE. Although, in the strong coupling limit, one needs to consider counter-rotating terms in the interaction Hamiltonian [37], in which there is still no analytically exact solution [38]. Instead of pursuing a full consideration, left for future work, we demonstrate here RWA, gives consistent results for the structure considered in this work. Moreover, we are interested in intensities but not in the correlations, and we replace the operators \hat{a}_i and $\hat{\rho}_{ij} = |\hat{i}\rangle\langle\hat{j}|$ with complex numbers α_i and ρ_{ij} [39] respectively and the desired equations of motion can be obtained as

$$\dot{\alpha}_{GP} = -(i\omega_{GP} + \gamma_{GP})\alpha_{GP} - i\Omega_R^*\rho_{ge} + \varepsilon_L e^{-i\omega t}, \quad (3.4a)$$

$$\dot{\rho}_{ge} = -(i\omega_{eg} + \gamma_{eg})\rho_{ge} + i\Omega_R\alpha_{GP}(\rho_{ee} - \rho_{gg}), \quad (3.4b)$$

$$\dot{\rho}_{ee} = -\gamma_{ee}\rho_{ee} + i\{\Omega_R^*\alpha_{GP}^*\rho_{ge} - c.c\}, \quad (3.4c)$$

where γ_{GP} and γ_{eg} are the damping rates of the GP mode and of the off-diagonal density matrix elements of the QE, respectively. The values of the damping rates are considered as the same with previous section. The conservation of probability $\rho_{ee} + \rho_{gg} = 1$ with the diagonal decay rate of the QE $\gamma_{ee} = 2\gamma_{eg}$ accompanies Eqs.(3.4a-3.4c). In the steady state, one can define the amplitudes as

$$\alpha_{GP}(t) = \tilde{\alpha}_{GP}e^{-i\omega t}, \quad \rho_{ge}(t) = \tilde{\rho}_{ge}e^{-i\omega t}, \quad (3.5)$$

where $\tilde{\alpha}_{GP}$ and $\tilde{\rho}_{ge}$ are constant in time. By inserting Eq.(3.5) into Eqs.(3.4a-3.4c), the steady-state solution for the GP mode can be obtained as

$$\tilde{\alpha}_{GP} = \frac{\varepsilon_L[i(\omega_{eg} - \omega) + \gamma_{eg}]}{(\omega - \Omega_+)(\omega - \Omega_-) + i\Gamma(\omega)}, \quad (3.6)$$

where $\Omega_\pm = \delta_\pm \pm \sqrt{\delta_-^2 - |\Omega_R|^2 y + \gamma_{eg}\gamma_{GP}}$ defines hybrid mode resonances [40] and $\Gamma(\omega) = [\gamma_{eg}(\omega_{GP} - \omega) + \gamma_{GP}(\omega_{eg} - \omega)]$ with $\delta_\pm = (\omega_{GP} \pm \omega_{eg})/2$ and population inversion $y = \rho_{ee} - \rho_{gg}$ terms.

It is important to note that the results presented in Fig. 5 and Fig. 6 are the exact solutions of Eqs.(3.4a-3.4c). We study the steady-state in Eq.(3.6) to gain a better understanding over the parameters and avoid time consuming electromagnetic 3D simulations of the combined system. Moreover, we hereafter calculate the intensity of the GP mode in Eq. (3.4a), which is related to the absorption from the nanostructure [29], to compare the results with the electromagnetic 3D-simulations.

To find the modulation of the intensities of the hybrid modes in the presence of QE, we use different resonance values of the QE, $\lambda_{eg} = 2\pi c/\omega_{eg} = 1535$ nm 1500 nm 1400 nm in Fig. 5a. The quantitative results comparing with the numerical simulations in Fig. 4, which takes retardation effects into account, are obtained. We also show the evolution of the hybrid-modes by varying interaction strength $|\Omega_R|$ for zero detuning ($\delta_- = 0$) in Fig. 5b, and for highly off-resonant case in Fig. 5c. The strong coupling regime is reached if $\Omega_R^2 > (\gamma_{GP}^2 + \gamma_{eg}^2)/2$ [41], that is the coupling strength exceeds the sum of the dephasing rates. When QE and GP are resonant [see Fig. 5b] a dip starts to appear around $|\Omega_R| \approx \gamma_{GP}$. This can be also read from Eq. (3.6). That is when $\omega_{eg} = \omega_{GP} = \omega$, the Eq. (3.6) becomes $\tilde{\alpha}_{GP} \propto \gamma_{eg}/(|\Omega_R|^2 y + \gamma_{GP}\gamma_{eg})$. Since γ_{eg} is very small from other frequencies, with increasing $|\Omega_R|$, $\tilde{\alpha}_{GP}$ becomes smaller compared to without QE case. Beyond a point, where the transparency window appears [34], there emerge two different peaks centered at frequencies Ω_\pm . The separation becomes larger as the Ω_R increases.

This argument is not valid if GP and QE are highly off-resonant. In this case, to make second peak significant, the interaction strength has to be much larger than γ_{GP} [see Fig. 5c]. The dip can be seen at ω_{eg} , which is out of the GP resonance window and it may not be useful for practical applications. However, having sharp peak, due to strong coupling between off-resonant particles, can be

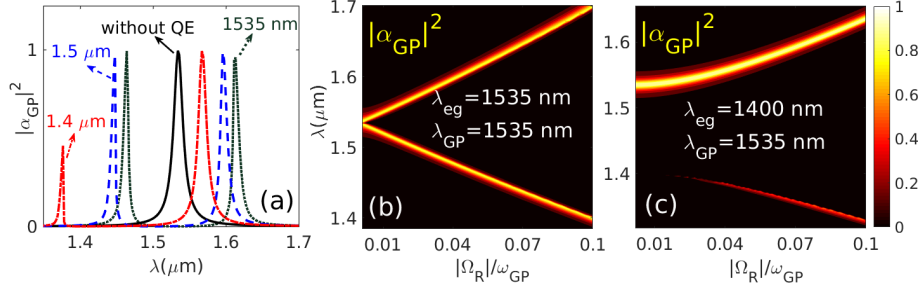


FIG. 5. The scaled absorption intensity of the GP ($|\alpha_{GP}|^2$) as a function of excitation wavelength λ , obtained from Eq. (3.4a-3.4c). (a) In the absence (black-solid) and in the presence of the QE having resonance at $\lambda_{eg} = 1535$ nm (dark gray-dotted), $\lambda_{eg} = 1500$ nm (blue-dashed) and $\lambda_{eg} = 1400$ nm (red-dashed-dotted) for a fixed coupling strength, $\Omega_R = 0.05 \omega_{GP}$. Variation of the resonance intensity of GP with excitation wavelength λ and coupling strength Ω_R for (b) $\lambda_{eg} = 1535$ nm and (c) $\lambda_{eg} = 1400$ nm. Here we use $\gamma_{GP} = 0.005 \omega_{GP}$ and $\gamma_{eg} = 10^{-5} \omega_{GP}$.

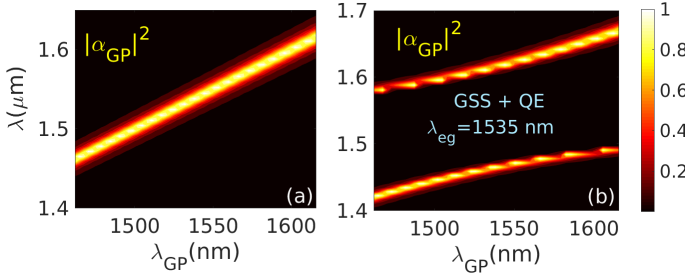


FIG. 6. The scaled field intensity of the GP ($|\alpha_{GP}|^2$) as a function of excitation wavelength λ and GP resonance λ_{GP} , when the GSS is alone (a) and with QE (b). We scale GP intensity with its maximum value and the parameters are used as: $\Omega_R = 0.1 \omega_{eg}$, $\gamma_{GP} = 0.01 \omega_{eg}$ and $\gamma_{eg} = 10^{-5} \omega_{eg}$.

very useful for the sensing. The reason for that it has smaller linewidth and can be tuned by changing chemical potential of the GSS. To show this, in Fig. 6 we plot the evolution of the field intensity of the GP ($|\alpha_{GP}|^2$) as a function of excitation wavelength λ and GP resonance λ_{GP} , when graphene is alone Fig. 6a and with QE Fig. 6b. It can be seen from Fig. 6b that it is possible to control the positions and linewidths of the hybrid resonances by varying the value of the chemical potential. The similar behaviour is also shown in MNPBEM simulation [see Fig. 3].

IV. CONCLUSIONS

In summary, we investigate the optical response of the GPs for the spherical shell geometry in the presence and absence of the QE. We show that there is a tunability of the optical response of the GSS through changing the value of the chemical potential and its radius. For the combined system of the QE covered with a graphene layer, we observe a splitting in the absorption band. This is due to the strong coupling regime where splitting of up to 80 meV are observed in a single QE limit. We also discuss the case when the QE and GP are off-resonant, and observe that the system can hold strong coupling. The results of the theoretical model, we present here, support the exact solutions of the 3D-Maxwell equations obtained from MNPBEM simulations.

Our results can contribute to controlling light-matter interactions at the nanometer length scale and find potential from all-optical switch nonlinear devices to sensing applications with current experimental capabilities for fabrication. Having extreme field confinement, device tunability and low losses makes such structures even more attractive.

ACKNOWLEDGMENTS

MG, VK and MET acknowledge support from TUBITAK Grant No. 117F118. MET acknowledges support from TUBA-GEBIP fund.

-
- [1] Andre K Geim and Konstantin S Novoselov, “The rise of graphene,” in *Nanoscience and Technology: A Collection of Reviews from Nature Journals* (World Scientific, 2010) pp. 11–19.
- [2] Jianing Chen, Michela Badioli, Pablo Alonso-González, Sukosin Thongrattanasiri, Florian Huth, Johann Osmond, Marko Spasenović, Alba Centeno, Amaia Pesquera, Philippe Godignon, *et al.*, “Optical nano-imaging

- of gate-tunable graphene plasmons,” *Nature* **487**, 77 (2012).
- [3] Zhe Fei, AS Rodin, GO Andreev, W Bao, AS McLeod, M Wagner, LM Zhang, Z Zhao, M Thieme, G Dominguez, *et al.*, “Gate-tuning of graphene plasmons revealed by infrared nano-imaging,” *Nature* **487**, 82 (2012).
- [4] Zheyu Fang, Sukosin Thongrattanasiri, Andrea

- Schlather, Zheng Liu, Lulu Ma, Yumin Wang, Pulickel M Ajayan, Peter Nordlander, Naomi J Halas, and F Javier García de Abajo, “Gated tunability and hybridization of localized plasmons in nanostructured graphene,” *ACS nano* **7**, 2388–2395 (2013).
- [5] M Gullans, DE Chang, FHL Koppens, FJ García de Abajo, and Mikhail D Lukin, “Single-photon nonlinear optics with graphene plasmons,” *Physical review letters* **111**, 247401 (2013).
- [6] F. Javier García de Abajo, “Graphene Plasmonics: Challenges and Opportunities,” *ACS Photonics* **1**, 135–152 (2014), arXiv:1402.1969.
- [7] Jacob B. Khurgin and Greg Sun, “Impact of surface collisions on enhancement and quenching of the luminescence near the metal nanoparticles,” *Optics Express* **23**, 30739 (2015).
- [8] Long Ju, Baisong Geng, Jason Horng, Caglar Girit, Michael Martin, Zhao Hao, Hans A Bechtel, Xiaogan Liang, Alex Zettl, Y Ron Shen, *et al.*, “Graphene plasmonics for tunable terahertz metamaterials,” *Nature nanotechnology* **6**, 630 (2011).
- [9] K S Novoselov, “Electric Field Effect in Atomically Thin Carbon Films,” *Science* **306**, 666–669 (2004).
- [10] A N Grigorenko, M Polini, and K S Novoselov, “Graphene plasmonics,” *Nat. Photon.* **6**, 749–758 (2012).
- [11] Tony Low and Phaedon Avouris, “Graphene plasmonics for terahertz to mid-infrared applications,” *ACS Nano* **8**, 1086–101 (2014).
- [12] Chenguang Liu, Zhenning Yu, David Neff, Aruna Zhamu, and Bor Z Jang, “Graphene-based supercapacitor with an ultrahigh energy density,” *Nano letters* **10**, 4863–4868 (2010).
- [13] Meryl D Stoller, Sungjin Park, Yanwu Zhu, Jinho An, and Rodney S Ruoff, “Graphene-based ultracapacitors,” *Nano letters* **8**, 3498–3502 (2008).
- [14] Jung-Soo Lee, Sun-I Kim, Jong-Chul Yoon, and Ji-Hyun Jang, “Chemical vapor deposition of mesoporous graphene nanoballs for supercapacitor,” *ACS nano* **7**, 6047–6055 (2013).
- [15] Wen-Chun Yen, Yu-Ze Chen, Chao-Hui Yeh, Jr-Hau He, Po-Wen Chiu, and Yu-Lun Chueh, “Direct growth of self-crystallized graphene and graphite nanoballs with ni vapor-assisted growth: From controllable growth to material characterization,” *Scientific reports* **4**, 4739 (2014).
- [16] Thomas Christensen, Antti-Pekka Jauho, Martijn Wubs, and N. Asger Mortensen, “Localized plasmons in graphene-coated nanospheres,” *Physical Review B* **91**, 125414 (2015).
- [17] Tingting Bian, Railing Chang, and PT Leung, “Optical interactions with a charged metallic nanoshell,” *JOSA B* **33**, 17–26 (2016).
- [18] Frank H L Koppens, Darrick E Chang, and F Javier García de Abajo, “Graphene plasmonics: a platform for strong light-matter interactions,” *Nano Lett.* **11**, 3370–7 (2011).
- [19] Giuseppe Toscano, Søren Raza, Wei Yan, Claus Jepsen, Sanshui Xiao, Martijn Wubs, Antti-Pekka Jauho, Sergey I Bozhevolnyi, and N Asger Mortensen, “Nonlocal response in plasmonic waveguiding with extreme light confinement,” *Nanophotonics* **2**, 161–166 (2013).
- [20] Yilei Li, Hugen Yan, Damon B Farmer, Xiang Meng, Wenjuan Zhu, Richard M Osgood, Tony F Heinz, and Phaedon Avouris, “Graphene plasmon enhanced vibrational sensing of surface-adsorbed layers,” *Nano letters* **14**, 1573–1577 (2014).
- [21] Osman Balci, Nurbek Kakenov, Ertugrul Karademir, Sinan Balci, Semih Cakmakcapan, Emre O Polat, Humeyra Caglayan, Ekmel Özbay, and Coskun Kocabas, “Electrically switchable metadevices via graphene,” *Science advances* **4**, eaao1749 (2018).
- [22] L Gaudreau, K J Tielrooij, G E D K Prawiroatmodjo, J Osmond, F. J. García de Abajo, and F H L Koppens, “Universal Distance-Scaling of Nonradiative Energy Transfer to Graphene,” *Nano Lett.* **13**, 2030–2035 (2013).
- [23] K. J. Tielrooij, L. Orona, A. Ferrier, M. Badioli, G. Navickaite, S. Coop, S. Nanot, B. Kalinic, T. Cesca, L. Gaudreau, Q. Ma, A. Centeno, A. Pesquera, A. Zurutuza, H. de Riedmatten, P. Goldner, F. J. García de Abajo, P. Jarillo-Herrero, and F. H. L. Koppens, “Electrical control of optical emitter relaxation pathways enabled by graphene,” *Nat. Phys.* **11**, 281–287 (2015).
- [24] Joseph a. Treadway, Geoffrey F. Strouse, Ronald R. Ruminski, and Thomas J. Meyer, “Long-Lived Near-Infrared MLCT Emitters,” *Inorganic Chemistry* **40**, 4508–4509 (2001).
- [25] Jeffrey M Pietryga, Richard D Schaller, Donald Werder, Michael H Stewart, Victor I Klimov, and Jennifer A Hollingsworth, “Pushing the band gap envelope: mid-infrared emitting colloidal PbSe quantum dots,” *J. Am. Chem. Soc.* **126**, 11752–3 (2004).
- [26] Ulrich Hohenester and Andreas Trügler, “Mnpbem—a matlab toolbox for the simulation of plasmonic nanoparticles,” *Computer Physics Communications* **183**, 370–381 (2012).
- [27] Denis G. Baranov, Martin Wersäll, Jorge Cuadra, Tomasz J. Antosiewicz, and Timur Shegai, “Novel Nanostructures and Materials for Strong Light-Matter Interactions,” *ACS Photonics* **5**, 24–42 (2018).
- [28] a Manjavacas, F J García de Abajo, and P Nordlander, “Quantum plexcitonics: strongly interacting plasmons and excitons,” *Nano letters* **11**, 2318–23 (2011).
- [29] Longfei Wu, Hongbin Feng, Mengjia Liu, Kaixiang Zhang, and Jinghong Li, “Graphene-based hollow spheres as efficient electrocatalysts for oxygen reduction,” *Nanoscale* **5**, 10839 (2013).
- [30] Marinko Jablan, Hrvoje Buljan, and Marin Soljačić, “Plasmonics in graphene at infrared frequencies,” *Phys. Rev. B* **80**, 245435 (2009).
- [31] L A Falkovsky, “Optical properties of graphene,” *J. Phys.: Conf. Ser.* **129**, 012004 (2008).
- [32] B Wunsch, T Stauber, F Sols, and F Guinea, “Dynamical polarization of graphene at finite doping,” *New J. Phys.* **8**, 318–318 (2006).
- [33] Ashkan Vakil and Nader Engheta, “Transformation Optics Using Graphene,” *Science* **332**, 1291–1294 (2011), arXiv:1101.3585.
- [34] Xiaohua Wu, Stephen K Gray, and Matthew Pelton, “Quantum-dot-induced transparency in a nanoscale plasmonic resonator,” *Optics express* **18**, 23633–23645 (2010).
- [35] Reshmi Thomas, Anoop Thomas, Saranya Pullanchery, Linta Joseph, Sanoop Mambully Somasundaran, Rotti Srinivasamurthy Swathi, Stephen K Gray, and K George Thomas, “Plexcitons: the role of oscillator strengths and spectral widths in determining strong coupling,” *ACS nano* **12**, 402–415 (2018).
- [36] MD Leistikow, Jeppe Johansen, AJ Kettelarij, Peter

- Lodahl, and Willem L Vos, “Size-dependent oscillator strength and quantum efficiency of cdse quantum dots controlled via the local density of states,” *Physical Review B* **79**, 045301 (2009).
- [37] Marlan O Scully and M Suhail Zubairy, “Quantum optics, Cambridge Univ. Press,” (1997).
- [38] CJ Gan and Hang Zheng, “Dynamics of a two-level system coupled to a quantum oscillator: transformed rotating-wave approximation,” *The European Physical Journal D* **59**, 473–478 (2010).
- [39] Malin Premaratne and Mark I Stockman, *Adv. Opt. Photon.*, Vol. 9 (2017) pp. 79–128.
- [40] Parinda Vasa and Christoph Lienau, “Strong light–matter interaction in quantum emitter/metal hybrid nanostructures,” *Acs Photonics* **5**, 2–23 (2017).
- [41] P Törmä and William L Barnes, “Strong coupling between surface plasmon polaritons and emitters: a review,” *Reports on Progress in Physics* **78**, 013901 (2014).